CROATICA CHEMICA ACTA CCACAA **65** (2) 379–409 (1992)

ISSN 0011-1643
UDC 541.1
CCA–2066

Original Scientific Paper

Fractal Structures and Their Effects on the Dynamics of Supramolecular Aggregates Studied by Light and Thermodynamic Measurements

Francesco Mallamace

Dipartimento di Fisica dell'Universita' di Messina, I-98166, Vill. S. Agata C.P. 55 (Messina) Italy

and

Norberto Micali

Istituto di Tecniche Spettroscopiche del C.N.R., I-98166, Vill. S. Agata (Messina) Italy

Received January 2, 1992

We report a review on light scattering, viscosity, sound propagation and calorimetric data in aggregating disperse systems, *i.e.* colloidal suspensions of polystyrene latex spheres and water in oil microemulsions. By elastic (intensity) and quasielastic light scattering (dynamics) direct information is obtained on aggregated clusters being built with a fractal structure and on the corresponding different kinetic mechanisms. In particular, dynamic data, showing a well-defined scaling behaviour in the measured mean linewidth, confirm the picture proposed by intensity data and allow a rough estimate of the cluster dimension. All the thermodynamic data, discussed in terms of a two- fluid model (suspending fluid and disperse interacting system), give evidence of the main role played by the attractive interparticle interaction. In fact, the typical features observed in viscosity and specific heat data and in the viscoelastic behaviour shown by these disperse systems can be connected to the long range structural order built by fractal aggregation processes. All the experimental data are consistent with the Derjaguin-Landau-Verwey-Overbeek theory on colloidal stability.

INTRODUCTION

Aggregation phenomena, *i.e.* the mechanisms of cluster formation from small isolated subunits, have recently been the subject of considerable interest in many fields of scientific research[1] and technology, such as physics, chemistry, biology, material science and in all kinds of nucleation phenomena at phase transition. In particular, on the basis of such studies, the physics and chemistry of colloids, polymers and gels

have been greatly improved and now constitute a proper method for the analysis of many interdisciplinary processes that are fundamental to immunology, biotechnical and biomedical sciences. Starting from the pioneering works of von Smoluchowsky[2] concerning the binary collision model on colloids aggregation and Verwey and Overbeek[3] theory of colloids stability, the mechanisms of particles aggregation have been intensively studied experimentally, theoretically and by computer simulation. The structural properties (shape and size) of such supramolecular aggregates can be utilized to obtain a clear display of the typical features in an aggregation process such as self-similarity, scaling, and universality,[4] several mechanisms of aggregation and growth can produce fractal objects, which look the same whether observed at a larger or a smaller scale. Since the use of the concepts of fractal geometry can describe clusters formed under a wide variety of conditions leading to many different studies aimed at a better understanding of the kinetics and structure of colloidal aggregates, fractal geometry actually constitutes an active and attractive area of research. The discovery of Witten and Sander[5] of a simple diffusion limited aggregation model (DLA), in which particles are added to a growing cluster via random walk trajectories leading to tenuous fractal structures, can be considered the starting point for several different growing processes (*e.g.* lattice animals, diffusion limited, percolation, reaction-limited and diffusion-limited cluster-cluster aggregations). These structures are described in terms of the fractal dimension D (Hausdorff dimension), which quantifies the way in which mass M of a cluster increases with its length R ($M \sim R^D$).[6] Growing processes, as shown from theory and modelling, have been used to predict the modes of clustering and aggregate growth. Such different aggregation models differ in D, so that the fractal dimension contains information about such mechanisms.[4]

Specifically for colloidal systems,[7,8] the growth of clusters can be classified into two distinct classes: reversible (reversible flocculation RF) and irreversible aggregation; in the latter case, in contrast to the former, after sticking together, the clusters cannot be separated into constitutive monomers. Both distinct classes can be accounted for in terms of the interparticle potential between two monomers which, as known, is constituted by the sum of an attractive and a repulsive contribution. In the case of irreversible phenomena, we can distinguish[8] between a reaction limited aggregation (RLA) and a diffusion limited cluster-cluster aggregation (DLCCA).

The DLCCA model, which can be considered an evolution of DLA, developed independently by Meakin and by Kolb, Botet and Jullien, can be explained as follows:[5,9,10] a particle is placed at the origin of a lattice; a second one, placed at a random site, at a given distance from the origin, walks randomly until it visits a site adjacent to the first one. Then, the walking particle becomes part of a cluster and so on. This cluster can diffuse, continuing to grow for successive aggregations with other clusters or single particles. In the RLA model, the aggregation process starts when the constitutive monomer is somehow activated:[11] its mechanism is less known and theoretical attempts have been recently made to understand it in terms of kinetic rate equations.[12] Very recently,[13] for this growth kinetics, the effects of attractive and repulsive contributions in the interparticle interaction have been studied. Interactions with a magnitude of k_BT (k_B being the Boltzmann constant and T the temperature) have important effects both in the aggregate structures and in the dynamics of aggregation. Attractive interactions lead to a more compact structures and repulsive interactions lead to a less compact one with lower effective dimensionality. As far as RLA is concerned, it is characterized by a fractal dimension $D = 1.2 \pm 0.1$ which has been directly measured in some experiments.[11] The study of the density correlation function for

DLCCA by computer simulation[9,10] and experimental results[11,8] give a fractal dimension $D = 1.75 \pm 0.1$. In such a case, the same exponent[8] characterizes the increase with time of the cluster size $R \sim \tau^{1/D}$. Both aggregation processes and their properties are well characterized and properly discussed in the works of P. Meakin and especially in the one reported in this issue.

Polystyrene-water solutions are a very interesting colloidal system because they show both mechanisms of aggregation; in fact, by changing the ionic strength, their reversible processes become irreversible. Dynamic light scattering experiments have shown that these solutions have a colloidal nature and reach RLA irreversible coagulation by passing through a phase of RF aggregation and subsequently pass to DLCCA aggregation.[8] The aggregation rate (strongly dependent on the radius of the particles), which can be calculated in terms of the DLVO (Derjaguin, Landau, Verwey and Overbeek)[3,14] theory, as a function of the salt concentration c, takes into account the different aggregation mechanisms. The entire process is attributed to the gradual decrease in the repulsive part of the pair potential. In fact, a single particle has a net surface charge resulting from the partial dissociation of protons in the surface carboxyl groups. This repulsive part of the potential can be shielded by adding some salt. In particular, at a lower salt content, the ionic strength is very low and the system is in the RF reversible regime; for a moderate salt content, usually $c \geq 0.1$ mol/l, the system passes into the irreversible aggregation regime. This is characterized by the presence of two different kinetics, namely the RLA ($0.1 \leq c \leq 1$ mol/l) and the DLCCA ($c > 1$ mol/l); in the first case, the dynamics of the cluster growth is slow while, in the second one, it is fast. In this latter case, the experimental results are well described using scaling arguments in a numerical solution of the Smoluchowski equation for diffusion limited cluster-cluster aggregation, which gives $R \sim \tau^{1/D}$ in the asymptotic time regime.

Another interesting system, in which well defined structures are originated and which can be considered as colloidal, is represented by microemulsion in the thermodynamic stable phase of water droplets dispersed in an oil medium (water in oil microemulsions). As shown by small angle neutron scattering in this thermodynamic phase, the packing fraction of the droplets, keeping their size constant, can be easily changed, giving rise to a very dense liquid system with interacting particles.[15] The interparticle potential function is similar in form to those of DLVO theory and has a repulsive hard-core plus a Yukawa tail, representing the attractive interaction. This interaction gives rise to very interesting phenomena, like a phase transition with an upper cloud point temperature[16] and, in particular, to an aggregation process by which fractal percolating clusters are built.[17] The overall behaviour, as a function of ϕ and T, of the percolation transition (PT) has been clarified by means of electrical conductivity and dielectric constant measurements, also detailing the temperature and concentration position of the percolation threshold.[18] A static percolation picture holds above the percolation threshold while below a dynamic one. In the dynamic percolation regime, the droplets show a connectivity increasing with the building of transient fractal clusters.[17] Therefore, microemulsions can constitute a model system to study experimentally the percolation kinetics of clustering, the corresponding structure and dynamic properties. The percolation model, although one of the most important models in statistical physics, which has been used to represent a broad variety of structures and of associated dynamical phenomena including phase transitions and polymers physics, has a very simple definition.[19] In fact, it can be represented by the following picture: in a large lattice, every site can be randomly occupied with probability p, and randomly empty

with probability $(1-p)$. A cluster can be identified as a group of occupied neighbouring sites. This implies that every site of a cluster is connected with every site of the same cluster by at least one chain of sites such that neighbouring sites and chains are only one lattice constant apart. Occupied sites on different clusters are not connected by such chains. For a small p, it is unlikely that a large cluster exists but increasing this occupation probability, the number of large clusters increases and when p reaches a critical value p_c (called percolation threshold), one of the clusters, the largest (incipient infinite or spanning cluster), extends across the entire lattice and will touch all the opposite sides of the system. This spanning cluster (for $p = p_c$) occupies only a negligible fraction of occupied sites. $p = p_c$ being a critical point, the behaviour of a percolating system near the threshold can be characterized in terms of a variety of critical exponents.[20] Near the threshold, the system can be characterized by a correlation length ξ. It has been shown, in terms of this quantity, that fractals geometry can be used to describe the structures generated by this model[20] and, for three dimensional percolating clusters, numerical simulations indicate a fractal dimension $D = 2.5$.

It is well known that scattering techniques are a powerful tool for studying fractal structures. Depending on the characteristic length scale to be observed and on the nature of the aggregate, it is possible to use neutron, X- ray, and light scattering. It can be shown that the scattered intensity, on a length much smaller than the cluster radius, is related to the transfer wave vector, k ($k = 4\pi n\lambda^{-1}\sin(\theta/2)$, through the simple relation[11,12] $I(k) \propto k^{-D}$. This power law relation for the scattered intensity provides a simple and accurate experimental method for determining the fractal dimension. Dynamical light scattering, by means of the photon correlation spectroscopy (P.C.S.), provides a microscopic probe of the dynamics of clusters with fractal structures; in fact, the mean decay rate (first cumulant) of the intensity autocorrelation function in such aggregated systems, which are fractal over dimensional scales comparable to the wavelength of light, scales like k^3. As predicted by the kinetic models for random aggregation in terms of scaling arguments,[21] the kR dependence of the linewidth is important because three dynamical regimes will be observed depending on the value of kR; for $kR \ll 1$, the fluctuations in concentration relax by the center of mass motion so that the linewidth shows the well known k^2 dependence; for $kR \gg 1$, this scaling law predicts a k^3 dependence for $\langle\Gamma\rangle$, so that in this region it is possible to probe the fractality of the clusters by intensity measurements. At $kR = 1$, a crossover is observed at the regime where $\langle\Gamma\rangle \sim k^3$.

The aim of this work is to report several studies of the aggregation process in some colloidal solutions, in particular polystyrene latex water suspension as a function of the salt concentration (ionic strength) and in water in oil microemulsions as a function of droplet volume fractions and temperature. In order to obtain a detailed view of the growth mechanism in these supramolecular systems, we report many of the experimental results that will be discussed in terms of the current models of aggregation phenomena. In particular, we are interested to show how the structure of such systems influences, in a direct way, their dynamics. For both systems, we report experimental results of the scattered intensity and the mean linewidth, obtained as the first cumulant of the intensity correlation function, as a function of different scattering angles. In the first case, we have a direct information about the fractal dimension; in the second one, the information concerns the k dependence of the average linewidth and gives detailed information about the dynamic properties of such colloidal systems and about their different kinetics growth. Namely, RLA and DLCCA for polystyrene suspensions and percolation for microemulsions. For this latter system, we report also

the results of Brillouin scattering, viscosity data and calorimetric measurements that explain the role of fractal structures on thermodynamical properties such as sound velocity, viscosity and specific heat. In particular, it is important to see how the structural relaxation of such a strongly interacting system for high packing fractions is connected to a well defined viscoelastic behaviour when cluster aggregates of tenuous structure are built up.

AGGREGATION PROPERTIES OF COLLOIDAL PARTICLES

It is important, at this point, to discuss the aggregation properties of the studied colloidal systems. Polystyrene water suspensions present both the reversible (RF) and irreversible kinetics of aggregation; the latter process exists in two regimes, a slow reaction limited regime (RLA) (characterized by a fractal dimension D ranging from 2 to 2.2) and a fast regime, which is diffusion limited (DLCCA), with $D = 1.75$. Water in oil microemulsions shows a percolation transition PT with $D = 2.5$. Both the reversible and irreversible aggregations in charged colloids and the aggregation effects, which start percolation clustering in microemulsions, can be explained and directly connected by the DLVO theory[3,14] of colloidal stability in terms of the interaction potential among two monomers. The pair potentials are similar in form for a colloidal suspension, as polystyrene latex particles, and for a microemulsion system; in fact, in the first case, it results in a long range repulsive shielded ionic interaction $V_R(r)$ plus an attractive short ranged van der Waals-London interaction $v_A(r)$; for microemulsion water droplets, it is made up of a repulsive hard core and a Yukawa tail representing a long range attractive contribution. As pointed out by the DLVO theory, these two contributions can be added giving: $V_T(r) = V_R(r) + V_A(r)$. For charged particles like polystyrene latex colloids, when the radius R_o of the constitutive particles is greater than the inverse of the Debye screening length κ ($R_o\kappa \gg 1$), the repulsive contribution is:

$$V_R(r) = 2\pi\varepsilon\psi_o^2 \ln\left(1 + \exp[-2\kappa R_o(r_o - 1)]\right) \tag{1}$$

while for $\kappa R_o \ll 1$, we have:

$$V_R(r) = \frac{4\pi\varepsilon\psi_o^2}{r} \exp(-\kappa r_o) \tag{2}$$

where $r_o = r/2R_o$ and r is the distance between the centers of the particles, ε is the dielectric constant of the structureless solvent medium, κ the inverse of the Debye screening length is

$$\kappa = \left(\frac{2e^2N \cdot 10^3}{\varepsilon k_B T} I\right)^{\frac{1}{2}} \tag{3}$$

where e is the electron charge, N the Avogadro number and I the ionic strength calculated including the total concentration n of the free-state (diffusible) cation and anion in the solution; in particular, we consider $n = n_c + n_s + n_o$, where n_c is the concentration of counterions, n_s the ions concentration due to the external added salt and n_o the hydrogen and hydroxide ions from the water dissociation, and $\psi_.$ is the particle surface potential related to the charge Z, due to the ionizable sites, on the colloidal particle, which for small values of κ ($\kappa R_o \leq 6$) can be written as:

$$\psi_o = \frac{Z}{4\pi\varepsilon R_o (1 + \kappa R_o)} \tag{4}$$

The attractive potential is:

$$V_A(r) = -\frac{A}{12}\left(\frac{1}{r_o^2 - 1} + \frac{1}{r_o^2} + 2\ln(1 - r_o^{-2})\right) \tag{5}$$

where $A = 3/4(\pi^2 q^2 h\nu\alpha^2)$ is the Hamaker constant,[22] with α the polarizability of the particle material, q the number of atoms per cm^3 and $h\nu$ is the energy corresponding to the main dispersion frequency ν in the dispersion spectrum of the atom (for our polystyrene particles its estimated value is $A \sim 0.08\times10^{-14}$ erg).

As it is well known the total DLVO potential $V_T(r)$ shows two minima with a barrier and its form depends on the ionic strength and on the particle size and, particularly, on κR_o.[3] The secondary minimum, which corresponds to the colloidal stable state and is usually obtained when the particles are further away (low number concentrations and low ionic strength), becomes more significant for larger particles and moves to smaller distances when the ionic strength is increased. When the particles are able to overcome the barrier, the primary minimum is reached, giving rise to irreversible aggregation phenomena. The secondary minimum position is, however, dependent on several physical quantities, such as the cited volume fraction and the ionic strength or the particle size or potential ψ_o or attraction constant A, as well as on the thermodynamic quantities such as temperature. Therefore, the colloidal state structure and its dynamics can assume different configurations and an appropriate calculation of the corresponding physical quantities can be made considering both the attractive and repulsive contributions to the DLVO potential form.

In evaluating the probability of particles to escape, by Brownian motion, the potential barrier can give a useful insight into the relaxation time of the colloid in its different aggregation phases. As shown by Chandrasekhar,[23] the analytical expression of potential $V(r)$ can be used to obtain the probability, per unit volume time, that particles initially in the secondary minimum escape over the potential barrier; assuming that the number of particles $N(t)$ in this minimum at a given time obeys the rate equation:

$$\frac{dN(t)}{dt} = -\frac{1}{\tau_E} N(t) \tag{6}$$

the tradition probability $P = 1/\tau_E$; can be written as:

$$P = \frac{(V_{min}'' \, V_{max}'')^{1/2}}{12\pi^2\eta} \, e^{-\Delta V/K_B T} \tag{7}$$

where ΔV is the height of the potential barrier, the V'' values are the second derivative of potential $V(r)$ calculated, respectively, in the position of the secondary minimum and in the position of the maximum (barrier position). In these terms the relaxation time τ_E is an exponential function of the height of the barrier that can give a simple interpretation of the physical situation. The reversible flocculation (metastable state) occurs for $k_B T \ll \Delta V$ and has a long decay time. Decrease of the height of the barrier with an increase of the ion concentration in the solution is equivalent to a decrease

of the metastable state lifetime, so that, at a given point, the system will quickly aggregate, passing from the reversible to the irreversible aggregation state. As shown by the results reported in the next section, this process can be studied by light scattering measurements. Evaluating from these the relaxation time τ_E as a function of the electrolyte content in the system, this point of view is also confirmed by the fit of the measured relaxation times with eq. (6). For the microemulsion, we explain that the aggregation phenomenon is originated in a similar way, in particular, as seen from light scattering, conductivity and viscosity measurement percolation is strongly dependent on the concentration and on temperature. Assuming a total interparticle potential analogous in form to those proposed by the DLVO theory, we can explain the obtained viscosity data and the overall viscoelastic behaviour of this and similar systems.

The presence in the region of an irreversible aggregation of two regimes, the reactive and the diffusive, with different aggregation kinetics, can be roughly explained, for polystyrene particles, in terms of the potential $V(r)$. The DLCCA kinetics is obtained for high electrolyte contents when the repulsive part of the potential $V_R(r)$ is completely shielded and the particles stick together after a diffusional motion by a simple contact. As the reaction limited kinetics RLA occurs in the intermediate salt concentration when a finite barrier in the potential is present, the aggregation process takes place after one simple, thermally activated, process. In any case, an accurate potential of the presence of the two different kinetics of aggregation in our system must be related to the influence of different effects with molecular origin in the parameters of the interaction potential, namely the Hamaker constant A and the surface potential ψ.. In particular, the Hamaker constant takes into account at last three different contributions:[24]

$$A = A_{11} + A_{22} - 2A_{12} \tag{8}$$

where A_{11} refers to the London dispersion forces between particles, A_{22} to the forces between water molecules, and A_{12} to the forces between the particles and water molecules.

It is generally assumed that A_{12} can be taken as the geometrical average of A_{11} and A_{22} so that

$$A = \left(A_{11}^{1/2} - A_{22}^{1/2}\right)^2 \tag{9}$$

It follows that A must always be positive and, therefore, in aggregation of colloidal particles, the London-van der Waals attraction term play the main role.

Several models,[25,26] including many-body effects and contributions from all interaction frequencies, have been developed in order to take into account the hydration and the solvent structure around the colloid particles and the effect of the salt concentration in the interaction potential $V(r)$, in particular in the Hamaker constant. These contributions, are refinements of the DLVO theory and do not affect its validity; in any case, the influence that such factors have on the coagulation is an open question. Recently, it has been pointed out that the deionized colloid shows extraordinary behaviour in structural[27] and dynamical properties;[28] in particular, in colloidal solutions similar to the ones studied in this work, viscosity measurements[29] give values much higher than those expected by Einstein's predictions and show a sharp decrease with the increasing of the concentration of the electrolyte. These results, relating to the dynamical and structural properties, are tentatively explained taking into account

the effects of the solvent and of external forces in the Debye cloud, indicating that molecular mechanisms of interaction between the particles must consider the effects of the solvent. In conclusion, a quantitative study of such contributions can give a clear and detailed explanation of the molecular origin of the presence of two different growth mechanisms, such as the RLA and DCLLA in the irreversible flocculation phase.

RESULTS AND DISCUSSION

A) Elastic Light Scattering (Scattered intensity)

A general and useful way of determining the fractal dimension of an aggregate observed in the real space uses the notion of the density correlation function which is directly connected with the measured scattered intensity. In fact, the measured intensity in a light scattering experiment can be written as:

$$I(k) \sim S(k)$$

where $S(k)$ is the structure factor, that is, the Fourier transform of the density correlation function $g(r)$. Since the fractal objects are self-similar structures [5.30] whose geometrical properties are scale invariant, the pair correlation function is homogeneous and can be written as:

$$\langle \rho(\lambda r_1)\, \rho(\lambda r_2) \rangle = \lambda^{-A} \langle \rho(r_1) \rho(r_2) \rangle \tag{10}$$

where $p(r)$ is the concentration of monomers at position r; this implies $\langle \rho(r_1)\rho(r_2) \rangle \sim |r_2 - r_1|^{-A}$. Exponent A is related to the fractal dimension D. If $N(R)$ is the number of monomers within radius R, then:

$$N(R) = \int_0^R \mathrm{d}^d r \langle \rho(0)\rho(r) \rangle / \langle \rho \rangle \sim \int_0^R \mathrm{d}^d r\, r^{-A} \sim R^{d-A} = R^D \tag{11}$$

where exponent d is the Euclidean space dimension and $d - A = D$ (analogously $M = R^D$ if M is the mass of the cluster). In terms of these arguments, it can be easily shown[31] that, for a fractal system, the structure factor satisfies the following general expressions:

$$S_M(k) = S(kR) \tag{12}$$

where S_M is the structure factor for a generic cluster of mass M, and in a d-dimensional expansion for $kR \gg 1$ (Porod region):

$$S(kR) = (kR)^{-D} \tag{12a}$$

Since the measured intensity $I(k)$ is proportional to the structure factor $S(k)$, we have:

$$I(k) \sim S(k) \sim k^{-D} \tag{13}$$

Therefore, we have the possibility of a direct measurement of the fractal dimension D (only for small distances compared with the radius of gyration of the fractal). If we use this latter simple relationship to measure D, a logarithmic representation of the measured scattered intensity $I(k)$, as a function of k, will be a straight line with slope D. However, for our system, we expect the constitutive particles to build up aggregates having a finite range of correlation ξ. It is shown[32] that this effect can be taken into account introducing an exponential cut-off factor $\exp(-r/\xi)$, analogous to the one used in critical phenomena, for the pair correlation function $g(r)$; in this way, the structure factor $S(k)$ assumes the following expression:

$$S(k) = 1 + \frac{1}{(kR_0)^D} \frac{D\Gamma(D+1)}{\left(1 + \frac{1}{k^2\xi^2}\right)^{(D-1)/2}} \sin[(D-1)\,\mathrm{tg}^{-1}(k\xi)] \tag{14}$$

where $\Gamma(x)$ is the gamma function. Eq. 14, which furnishes a simple and accurate method of determining the fractal dimension D and the value of ξ by intensity profiles, combines the fractal nature of the system whose pair correlation function decays like a power law for the self-similarity of its internal structure with the finite extension of the range of correlation ξ, which is taken into account by the use of the exponential cutoff. A very extended k range ($k < 1/\xi$ up to $k > 1/R_0$) is necessary for its complete application, compared with the one allowed by visible light measurements. For small k, $k\xi \ll 1$, Eq. 14 becomes

$$S(k) = \Gamma(D+1)\left(\frac{\xi}{R_0}\right)\left(1 - \frac{D(D+1)}{6}k^2\xi^2\right) \tag{15}$$

and the cutoff ξ reflects the finite overall size of the system and can correspond to the cluster size. In the range $1/\xi \ll k \ll 1/R_0$, *i.e.* on a length scale smaller than the cluster dimension and greater than the constitutive monomer (single particle in our case), we again have $S(k) \sim (kR_0)^{-D}$ and we obtain that the scattered intensity is related to the exchanged wavevector k, through the results of Eq. 13: $I(k) \sim k^{-D}$. This latter result outside the $k\xi \gg 1$ and $kR_0 \ll 1$ k limits, cannot be applied to the D determination. In any case, the k region, where Eq. 13 holds, is strongly dependent[32] on the ratio ξ/R_0, and a good determination of D is obtainable for $\xi/R_0 \sim 30$. In such a case, the obtained values of D can be directly connected to the peculiar aggregation kinetics. It has been shown, in terms of the scaling theory of the percolation clustering,[31] that when the system is highly polydispersed, the structure factor and, hence, the scattered intensity at the gel point obey the following relation:

$$I(k) \sim S(k) \sim k^{-\mu} \tag{16}$$

where $\mu = D(3 - \tau)$ and $\tau = 2.2$ is the percolation exponent that can be obtained from the theory.[20] For percolation systems and in particular for dense microemulsions, Tartaglia *et al.*[33] have recently developed a model for the scattered intensity in percolating system giving the form that corresponds to eq. 14. This calculation uses the size distribution function $N(M)$ for the percolation cluster containing M particles. As it is well known, such a function has the scaling form[19] $N(M) = M^{-\tau}f(M^{\sigma}/s^{\sigma})$, characterized by the two exponents τ and σ, and s has the meaning of the average number of particles

in a cluster. Numerical simulations for three dimensional percolation indicate $D = 2.5$, a polydispersity exponent $\tau = 2.2$ and $\sigma = 0.45$.[19]

Now, we report some results obtained for polystyrene latex suspensions and microemulsions and describe the sample preparation and the experimental set-up, keeping in mind that great care must be taken in optical measurements to avoid dust contamination of the samples. The measurements were made at constant temperature in an optical thermostat allowing temperature regulation better than 10^{-2} °C. For latex solution, the stability of the solution was checked throughout a week by measurements of the mutual diffusion coefficient by dynamic light scattering. In such a case, the hydrodynamic radius corresponds to that of an isolated particle and no irreversible aggregation takes place.

Measurements of the scattered intensity as a function of the scattering angle θ (wave vector k) were carried out using a computer controlled goniometer, utilized in classical scattering geometry, with a 10 mW unimode He–Ne laser operating at a wavelength of 6328 Å as the light source. In order to observe fractal behaviour in the scattered intensity for the studied system it is important to assure the Porod conditions $kR > 1$. Therefore, an angular range $15° \leq \theta \leq 70°$, was chosen for polystyrene particles, corresponding to the k range $3.37\ \mu m^{-1} \leq k \leq 14.81\ \mu m^{-1}$; while for microemulsions the experimental angular range is $30° \leq \theta \leq 120°$, with a k that ranges in the interval $7.19\ \mu m^{-1} \leq k \leq 24.1\ \mu m^{-1}$, Such k intervals, available by the use of light scattering, are too narrow to accurately define a fractal behaviour; the region of self-similarity for fractal systems is usually observed on a larger scale of lengths. In fact, such a k interval is narrow for the application of eq. 14, which requires k ranges of several orders of magnitude; nevertheless, it is sufficient, by utilizing eq. 13, to point out the existence of a scaling behaviour. This problem can be overcome, as it can be seen from the next paragraph, by studying the k dependence of the mean linewidth $\langle\Gamma\rangle$.

For polystyrene colloidal systems, the salt concentration explored is $0.01 \leq c \leq 3$ mol/l, for $T = 25$ °C, which spans all the aggregation regimes. Intensity measurements are repeated at different times in order to study the kinetic behaviour of the aggregation processes of macromolecules; in the case of RF kinetics, complete aggregation is reached after several days. The microemulsion used in these experiments consisted of a mixture of AOT as surfactant, water and decane as oil. The samples were prepared using a well defined procedure.[15] The molar ratio water to surfactant was $X = H_2O/AOT = 40.8$, giving a mean radius of water droplets of about 50 Å with a polydispersity of the spherical particles of about 0.20. The concentration of microemulsion droplets was calculated at the sum of the volume fraction of water and surfactant added to the decane. The explored concentration range is $0.05 \leq \phi \leq 0.75$, where the microemulsions are of the water-in-oil type and where the mean radius remains constant and the droplet persists.[15]

Figure 1a presents some typical profiles, $\log I(k)$ *versus* $\log k$ for latex suspensions at salt concentrations $c = 0.075$ mol/l (a), 0.15 mol/l (b) and 1.5 mol/l (c) after the system has reached a stationary condition.[34] The continuous lines are the best fits of the experimental results by eq. 13. The plots are representative of different mechanisms of aggregation, in particular case (a) corresponds to the RF, case (b) to the RLA, and, finally, case (c) to the DLCCA, for cases (a) and (b) we have $D = 2.1 \pm 0.05$, while for (c) we have $D = 1.75 \pm 0.05$. In Figure 1b analogous results are reported for microemulsions at different volume fractions ϕ. In this case, the obtained values of the effective slope $\mu \approx 2.1$, at the percolating concentration $\phi = 0.56$, at $T = 25$ °C, are consistent with the percolation fractal clustering model. In fact, we have $D = 2.5$ and $\tau = 2.2$.

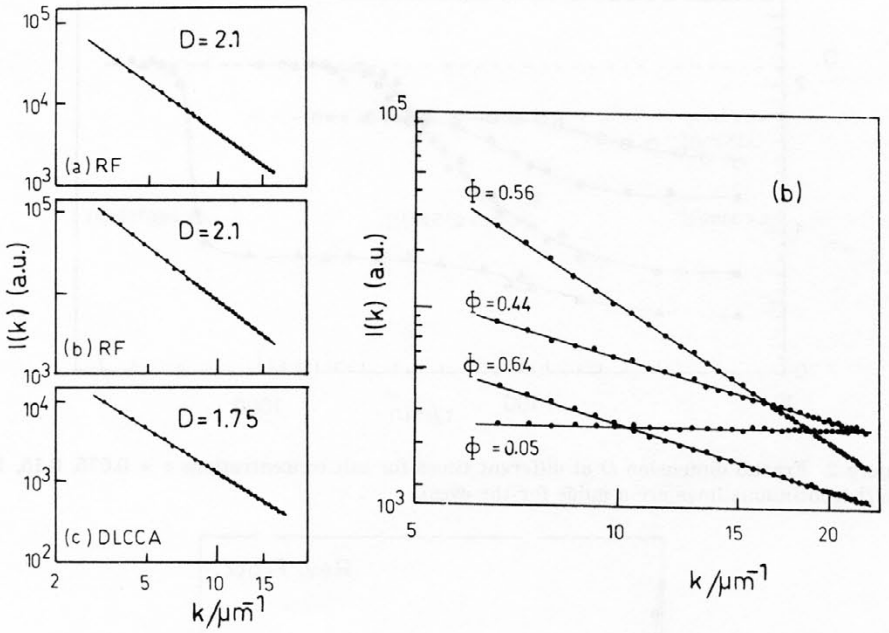

Figure 1a. Intensity profiles, $I(k)$ *versus* k, in the polystyrene latex suspension at salt concentrations c = 0.075 mol/l (a), 0.15 mol/l (b) and 1.5 mol/l (c). Experimental data are taken after the system has reached a stationary conditions. The continuous lines are the best fits of the experimental results eq. 13. Figure 1b. Analogous results for microemulsions at different volume fractions ϕ.

Figure 2 shows the measured slope (log I *vs.* log k) of the obtained intensity profiles at different times for salt concentrations c = 0.5 and 0.075 mol/l. As it can be seen, the complete aggregation is obtained at different times for different concentrations values. At high concentrations (c = 3 mol/liter), the kinetic regime is the DLCCA (D = 1.75±0.01) and the process is fast. The time behaviour of this regime is in close agreement with the numeric solution of the Smoluchowski equation for DLCCA aggregation.[8] At c – 0.15 mol/l, the system is in a slow regime and the obtained fractal dimension (D = 2.1±0.01) indicates an RLA aggregation. For c = 0.075 mol/l, the aggregation process is very slow, reversible flocculation (RF) occurs and the system exhibits evidence that complete aggregation is obtained passing through an »intermediate« state where we measure an »apparent« fractal dimension $D \sim 0.9$ for some days. The origin of such a behaviour, and in particular of the presence of a metastable state, is clear if we consider the description of reversible flocculation in terms of the DLVO theory. For very low salt concentrations, the relaxation time τ_E (see eq. 7) is very large because the particles stay in the secondary minimum for a long time. The value of $D \sim 0.9$ in the metastable region is clearly apparent and can be easily connected to the limited experimental k range used. As shown by the analysis of eq. 14, at a constant k range of measurement, for concentrations in which the ratio ξ/R_0 is small, measurement D is underestimated. This underestimation is more pronounced for smaller

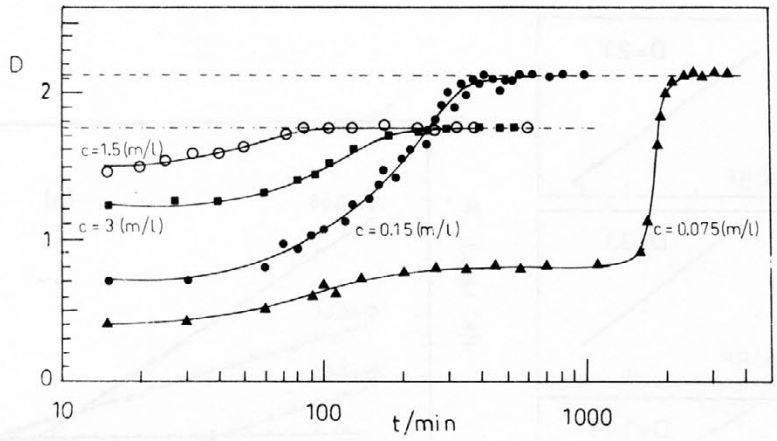

Figure 2. Fractal dimension D at different times for salt concentrations c = 0.075, 0.15, 1.5, 3 mol/l (continuous lines are a guide for the eyes).

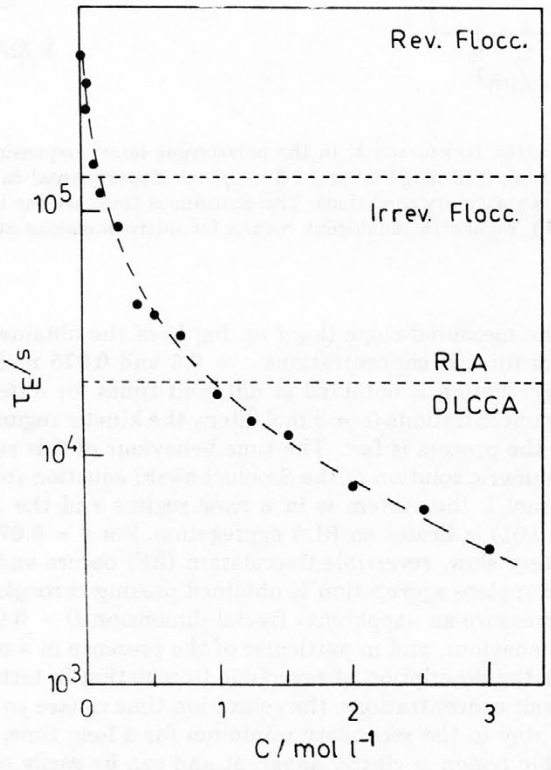

Figure 3. Time τ_E for complete aggregation as a function of salt concentration. The dashed line is the result of calculation, using eq. (7), of the inverse rate of passage above the potential barrier ($\tau_E = 1/P$).

values of ξ. The application of eq. 14 confirms this point of view. In fact, keeping the fractal dimension $D = 2.1$ constant, we obtain, as a result of the fitting of the data, in the metastable region that the value of ξ is of some thousands of Å, in particular, we have $\xi \sim 4$–6 time R_0. Such values of ξ are obtained with great uncertainty because for a correct determination of both D and ξ by scattering data, eq. 14 must be applied to a larger k interval than the one used. This picture is confirmed by the analysis of the dynamical data.

Finally, in Figure 3 we report the obtained time τ_E, defined as the inverse rate of passage above the potential barrier ($\tau_E = 1/P$), for complete aggregation as a function of the salt concentration. The dashed line represents the theoretical value obtained from eq. 7 with these values of the parameters: R_0 (radius of the particle) 425 Å, $\psi_0 = 7.2\times10^{-5}$ cgs units, $\varepsilon = 78.55$ and $T = 298$ °K; the Hamaker constant is $A = 0.043\times10^{-14}$, this value is calculated as $A = (A_{11}^{1/2} - A_{22}^{1/2})^2$ with A_{11} the value relative to the particle and A_{22} the value for water molecules; these values are obtained from literature data[8,35,36] $A_{11} = 8\times10^{-12}$ erg $A_{22} = 6\times10^{-13}$ erg. As it can be seen, the experimental results are in agreement with the calculation.

ii) Quasi-Elastic Light Scattering

We also carried out Quasi Elastic Light Scattering Measurements (Q.E.L.S.) for both systems in the same k range used for intensity measurements, by the homodyne technique (photon correlation spectroscopy), using a full correlator. The same scaling form used for the structure factor and precise models of kinetic growth for fractal aggregates can be used to render information about the dynamic properties of such structures. In a homodyne experiment, we measure the first cumulant of the autocorrelation function of the scattered field $g^{(1)}(k,\tau)$ which gives the mean decay rate, or Rayleigh linewidth; this quantity is proportional to the dynamic structure factor $S(k,\tau)$:[37]

$$\langle\Gamma\rangle = \frac{\mathrm{d}\ln g^{(1)}(k,\tau)}{\mathrm{d}\tau}\Big|_{\tau=0} = \frac{\mathrm{d}\ln S(k,\tau)}{\mathrm{d}\tau}\Big|_{\tau=0} \tag{17}$$

For branched polymers, the first cumulant is:[37]

$$\Gamma = -\frac{\mathrm{d}\ln S(k,\tau)}{\mathrm{d}\tau}\Big|_{\tau=0} = D_0 k^2 + A(kR)\theta \tag{18}$$

where θ is the rotational diffusion coefficient and $A(kR)$ an amplitude function. For aggregates which are essentially spherical in shape and for $kR \gg 1$, the rotational effects dominate Γ.

Since clusters of different sizes contribute to the experimentally observed first cumulant, we have a mean linewidth weighted by the number distribution of cluster sizes $P(M)$, [$P(M) = N(M)/c\,v$, where $N(M)$ is the number of aggregates of molecular weight M in the scattering volume v, and c is the mass concentration for unit volume. In any case, we have $\Sigma\, M\, P(M) = 1$]. In terms of the structure factor $S_M(k)$, for a cluster of molecular weight M [the scattering strength is proportional to $M^2 S_M(k)$], we have:

$$\langle\Gamma\rangle = \frac{\int M^2P(M)S_M(k)\,[D_0k^2 + A(kR)\theta]\,dM}{\int M^2P(M)S_M(k)\,dM} \tag{19}$$

The scaling form of the structure factor and precise models of kinetic growth suggest the form of $P(M)$, giving the solution of eq. 17. From the theoretical point of view, two different distributions of cluster sizes, calculated respectively from a percolation model and from the solution of the Smoluchowski equation in the kinetic cluster-cluster aggregation model, furnish an analogous result:[38]

$$\langle\Gamma\rangle = k^2D_zF(kR_z) \tag{20}$$

where D_z is the average cluster diffusion coefficient and R_z the average cluster radius of gyration, the function $F(kR_z)$ taking the internal modes into account. However, in contrast to the percolation model, the obtained function $F(kR_z)$ for the kinetic cluster-cluster aggregation is complex and not universal.[38] However, it is shown[14,31] that for $kR_z \ll 1$ $F(kR_z) = 1$ and $\langle\Gamma\rangle = k^2D_z$. Under these conditions, the intensity measurements are insensitive to the fractal nature of the system. The obtained diffusion coefficient is due to fluctuations in the concentration and, therefore, represents the cluster diffusion constant. In any case, the latter result cannot be directly applied to the measurement of the hydrodynamic radius ξ of the clusters by means of the well-known Einstein-Stokes relation because polydispersity effects and asymmetries in the clusters give smaller values in ξ.[39].

If our attention is restricted to the »Porod« regime $kR_z \gg 1$, scaling arguments[21] give $F(kR)_z \sim kR_z$ and, in this large kR_z limit, the mean linewidth $\langle\Gamma\rangle$ becomes independent of the correlation range:

$$\langle\Gamma\rangle \sim k^3 \tag{21}$$

This k^3 dependence could be experimentally tested and, as a consequence, the Porod regime can be studied by light scattering intensity experiments giving detailed information about the properties of the structures and about the growth mechanism determining them. When $kR_z \sim 1$, we are in the crossover regime and all the processes (centre of mass diffusion, rotation and configurational relaxation) have the same rate $\langle\Gamma\rangle_0 \sim 1/R_z^3$, where $\langle\Gamma\rangle_0$ is called the »fundamental relaxation rate«. The validity of such arguments can be observed in Figure 4 showing the normalized relaxation rate $\langle\Gamma\rangle/k^2$ *versus* kR_z for different macromolecular water solutions, *i.e.* lysozyme, BSA and DNA.[40] It is evident that, in the utilized k-range, these data indicate the condition $\langle\Gamma\rangle_{lys} \sim k^2$ for the lysozyme, for BSA and DNA, and the $\langle\Gamma\rangle \sim k^3$ case. For R_z, we have used the values of previous works,[41] that is 0.05 μm for lysozyme, 0.1 μm for BSA and 1μm for DNA while the corresponding hydrodynamic radii of single macromolecules are 25, 50 and 250 Å, respectively. At this point, it is important to stress that data corresponding to the dynamic behaviour are obtained considering only the first cumulant contribution whereas the entire measured correlation function can give information about a wide temporal range. Taking into account only the first cumulant analysis, the long term dynamics is neglected. These latter properties, *i.e.* the long time behaviour, can instead fournish significant physical information about aggregating systems like ours. In fact, in a very interesting recent paper,[34] it is shown that the use of percolation concepts allows calculation of the entire density-density correlation function that fits experimental data very well. In particular, it is shown that initially such a function

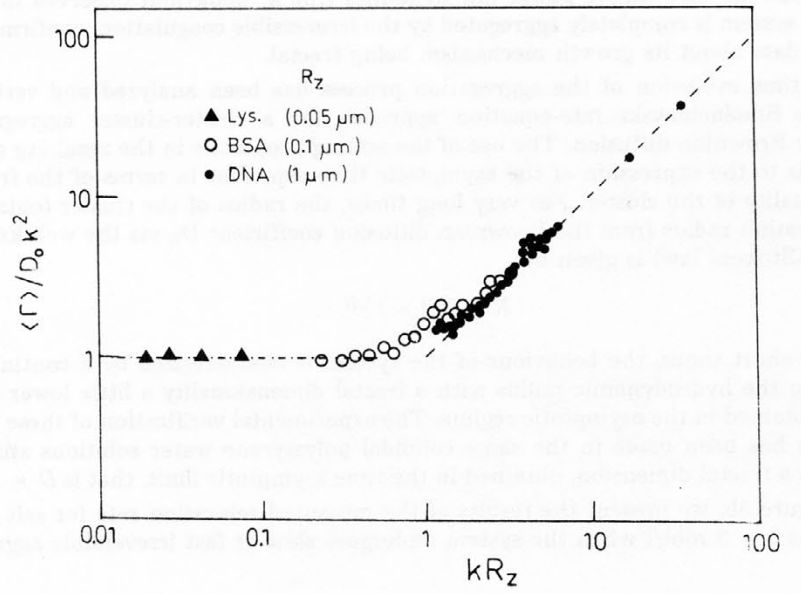

Figure 4. Normalized relaxation rate $\langle\Gamma\rangle/k^2$ for lysozyme, BSA and DNA water solutions.

decays exponentially and evolves continuously, increasing the time, into a stretched exponential asymptotical form typical of relaxation phenomena in complex fluid systems or strongly interacting colloidal systems.

In Figure 5a, we report the values of log $\langle\Gamma\rangle/k^2$ *versus* log k for two different ionic concentrations, namely c = 0.05 and 0.075 mol/l when the system undergoes the reversible flocculation regime (RF). For the salt concentration c = 0.05 mol/l (dotted lines), the data were taken just after the sample preparation (crosses) and after several days (full squares) when the system showed evidence that complete aggregation had been obtained.[34] In the first case, the measured linewidth shows a k^2 dependence while in the second case $\langle\Gamma\rangle \sim k^3$. For c = 0.075 mol/l, we report (continuous lines) the log $\langle\Gamma\rangle/k^2$ values just after the sample preparation (rhombs) and for several time intervals afterwards: 3 hours, 8 hours, and 12 hours. The log $\langle\Gamma\rangle/k^2$ values after couple aggregation (2×10^3 minutes) are also shown. In this case too, the mean linewidth shows the k^3 dependence when the irreversible aggregation takes place. The behaviour between these two extreme conditions is, in our opinion, very interesting. When the colloidal suspension is in the metastable state of reversible flocculation, the k dependence of the mean linewidth behaviour is intermediate between the Guinier ($\sim k^2$) and the Porod (k^3) regime. When the measured linewidth shows such a behaviour, the system is in the so-called crossover regime and, in analogy to the polymeric systems, all processes (centre of mass diffusion, rotation and configurational relaxation) present the same rate $\langle\Gamma\rangle_o$, called the fundamental relaxation rate. In this condition, we have $kR_z \sim 1$ and the extracted value for the gyration radius of the cluster has a value that is

of the same order of magnitude as that obtained from the intensity measurements, R_z ~ 5–8 times R_o. The simple power law dynamics (the k^3 behaviour observed in $\langle\Gamma\rangle$), when the system is completely aggregated by the irreversible coagulation, confirms the intensity data about its growth mechanism being fractal.

This time evolution of the aggregation process has been analyzed and verified[8] using the Smoluchowski rate-equation approach for a cluster-cluster aggregation limited by Brownian diffusion. The use of the scaling properties in the resulting equations leads to the expression of the asymptotic time exponent in terms of the fractal dimensionality of the cluster. For very long times, the radius of the cluster (obtained as the gyration radius from the Brownian diffusion coefficient D_B via the well known »Einstein-Stokes« law) is given by:

$$R \sim D_B^{-1} \sim t^{1/D} \tag{22}$$

while, for short times, the behaviour of the system is characterized by a continuous increase in the hydrodynamic radius with a fractal dimensionality a little lower than the one obtained in the asymptotic regime. The experimental verification of these time evolutions has been made in the same colloidal polystyrene water solutions studied here, with a fractal dimension, obtained in the time asymptotic limit, that is $D = 1.75$.

In Figure 5b, we present the results of the measured relaxation rate for salt concentrations $c = 3$ mol/l when the system undergoes slow or fast irreversible aggrega-

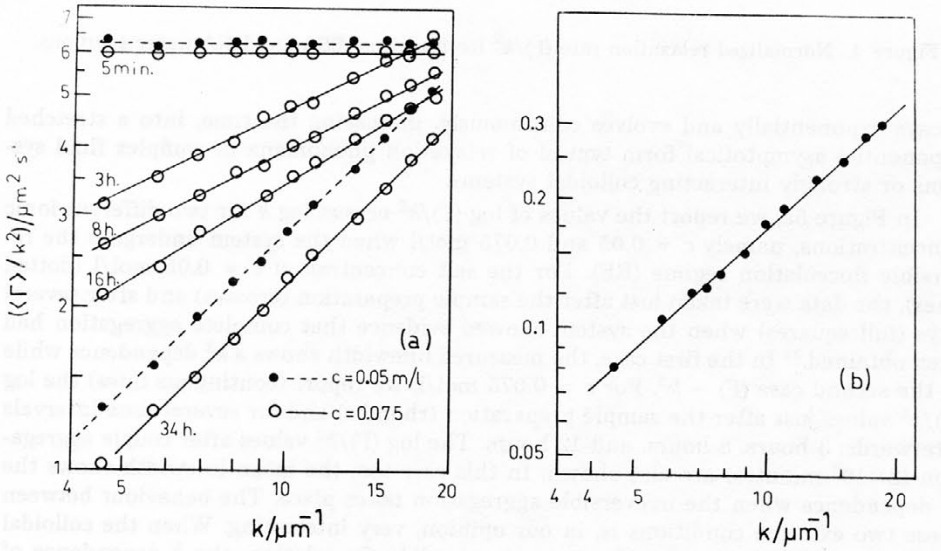

Figure 5 (a) Relaxation rate of the mean linewidth $\langle\Gamma\rangle/k^2$ *versus* for two different ionic concentrations, namely $c = 0.05$ and 0.075 mol/l, in the reversible flocculation regime (R.F.). For c = 0.075 mol/l the data are taken at different times after the sample preparation; data corresponding to 34 hours refers to complete aggregation; (b) Analogous result for salt concentration c = 3 mol/l, in which the system undergoes irreversible aggregation.

tion. As shown by intensity data, in this regime, the system shows both the kinetic growth RLA process for c = 0.15 mol/l (slow regime) and the DLCCA for c = 3 mol/l (fast regime). In the first case, we can measure the behaviour of the solution just after the sample preparation while in the second case, such a measurement is unreported since the aggregation process is very fast (about 15 minutes) and comparable with the time of the mean linewidth measurement. For both concentrations, in the aggregated phase, the $\langle\Gamma\rangle$ shows the well-known k^3 dependence indicating a fractal growth mechanism in agreement with the intensity data. Analogous behaviour has been determined for the dense microemulsion systems.[17]

iii) Thermodynamic Results (Viscosity, Brillouin and Calorimetric Results)

In the present and in the next sections we discuss, in particular for macroemulsions, how the presence of a self- similar structure in the system can determine the behaviour of thermodynamic quantities such as viscosity, hypersound velocity and specific heat. In the logarithm plot in Figure 6, the ratio (relative viscosity) of the measured microemulsion viscosity to decane viscosity η_0 ($\eta_s = \eta/\eta_0$) is shown for different concentrations as a function of T.[42] As it can be seen, the data show an increase

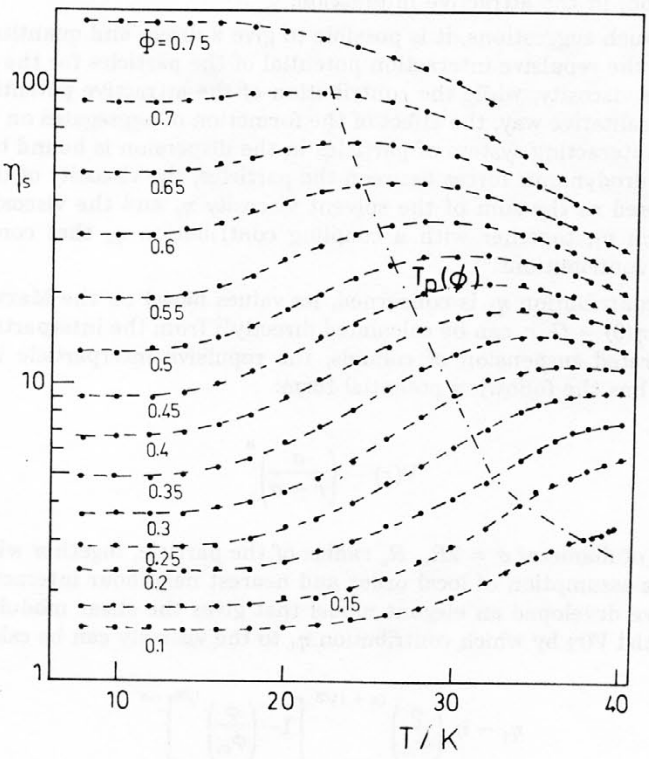

Figure 6. Plot of the relative viscosity η_S of a microemulsion system (AOT – decane – water) as a function of temperature and for different water volume fractions. The dotted point line, T_p, represents the percolation threshold.

in the viscosity, starting at about 25 °C for lower concentrations and about 12 °C for higher concentrations, with a maximum whose position is well defined for volume fractions $\phi > 0.25$. The temperature value of the maximum decreases when the concentration increases. For all concentrations, there is a lower temperature region where the relative viscosity is temperature independent; such a T interval is more extended for less concentrated microemulsions. The entire behaviour of the data points to some kind of thermally activated process. Furthermore, the percolation threshold line determined by conductivity data is presented (dotted line) as $T_p(\phi)$ in the same figure. It should be noted that $T_p(\phi)$ crosses the viscosity curves in their steepest rising part to the peaks. In agreement with analogous behaviour in polystyrene particles at moderate concentrations,[29] such a result seems to indicate that the lowest temperature behaviour of the viscosity can be exclusively ascribed to the packing effect. Furthermore, as analogous temperature effects, as kinks and maxima, have recently observed in colloidal solutions by several experiments[43,44] and have been qualitatively described, invoking aggregation processes originated by the attractive interactions, an analysis is possible of the reported viscosity, as due separately to two different contributions. One is related to the packing effect (temperature independent) and the other to the aggregation processes, well evidenced by the light scattering results, originating, like in the colloidal solution, in the attractive interaction.

Following such suggestions, it is possible to give a direct and quantitative account of the effect of the repulsive interaction potential of the particles for the packing contribution to the viscosity, while the contribution of the attractive potential takes into account, in a qualitative way, the effect of the formation of aggregates on the viscosity. Since such an interacting system of particles in the dispersion is bound to the solvent through the hydrodynamic forces between the particles, the viscosity of the dispersion can be considered as the sum of the solvent viscosity η_o and the viscosity of the interacting system η_1, together with a coupling contribution η_2 that contains all the hydrodynamic contributions.[34]

As far as contribution η_1 is concerned, its values based on the Maxwell model of viscoelasticity, $\eta(0) = G_\infty r$, can be calculated directly[46] from the interparticle potential. For a concentrated suspension of colloids, the repulsive interparticle interaction is dominant and has the following potential form:

$$V(r) \sim \left(\frac{\sigma}{r-\sigma}\right)^n \tag{23}$$

(a »hard« core of diameter $\sigma = 2R_o$, R_o radius of the particle, together with an inverse power). On the assumption of local order and nearest neighbour interactions, R. Buscall *et al.*[46] have developed an elegant model that gives the shear modulus directly in terms of potential $V(r)$ by which contribution η_1 to the viscosity can be calculated[45] as:

$$\eta_1 \sim \eta_o \left(\frac{\phi}{\phi_m}\right)^{(n+1)/3} \left[1-\left(\frac{\phi}{\phi_m}\right)^{1/3}\right]^{-n} \tag{24}$$

As the microemulsion potential (in the water-in-oil phase) is due to a hard core repulsion plus an attractive contribution,[15] we can consider that, in the temperature region where aggregation effects are absent, only the repulsion term contributes to η_1,

which can be quantified by eq. 24. Thus, the last equation can be used for an analysis of the viscosity at the lowest temperature. We have made the best fit of the data ascribed to the packing effects using the following expression:

$$\eta_S = 1 + \frac{1}{\eta_o}(\eta_1 + \eta_2) = (1 + 2.5\phi) + \left(\frac{\phi}{\phi_m}\right)^{n+1/3}\left[1 - \left(\frac{\phi}{\phi_m}\right)^{1/3}\right]^{-n} \quad (25)$$

using as free parameters the multiplicative constant A, the random close packing volume fraction ϕ_m, and the exponent of the potential form n and assuming that only the Einstein term[47] $(1+2.5\phi)$ contributes to η_2; the fit of the data is shown in Figure 7 and the obtained values for the parameters are: $A = 0.56$, $\phi_m = 0.81$ and $n = 1.97$.

These results are in agreement with the physical properties of water in oil microemulsion.[48] According to the general behaviour of colloidal systems, the only possible interaction is attractive plus a repulsive hard core. This last component contributes to the viscosity term η_1; as the droplets bear no net charge, the only possible one is a dipolar form, $n = 2$.

Finally, we discuss the effects of the aggregation process in the viscosity as due to the attractive potential. Since, in our model, the measured viscosity at $T = 10$ °C is completely attributed to the effect of repulsion of the particles, in order to obtain some insight into the effects of the attractive potential, we consider the excess of viscosity $\Delta\eta_s$ at different ϕ and against T, namely the difference between the viscosities measured at higher temperatures and their constant value for low T (10 °C). The result of this procedure is shown in Figure 8a. As it can be seen, for each volume fraction, we have curves with a well defined maximum, whose position is lowered in T, increasing ϕ. The $\Delta\eta_{SM}$ (the value of $\Delta\eta_S$ in correspondence to each maximum) increases its value, increasing ϕ up to $\phi \approx 0.55$, and then it decreases sharply.

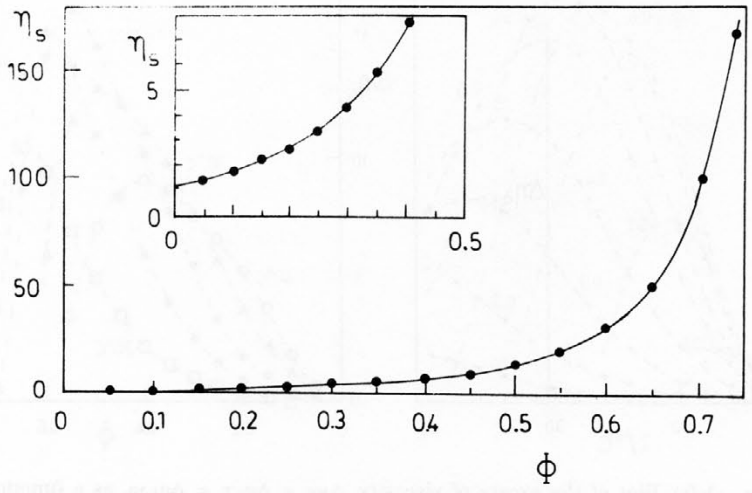

Figure 7. Best fit of low temperature (Tm ≤ 10 °C) relative viscosity experimental data (dot) with eq. 25.

Such behaviour in the excess of viscosity and its dependence on T and ϕ agree with the behaviour of concentrated suspension of colloidal particles and can be connected to the aggregation process. In particular, the presence in the system of large clusters with fractal geometry, built-up by a well defined aggregation process due to the attractive part of the potential, can explain, at least qualitatively, the presence of the maxima in the viscosity, in the $\phi < \phi_m$ region. Considering the diameter of constitutive monomers, σ in a cluster of radius R, the number of monomers $N(R)$ scales as:

$$N(R) \sim \left(\frac{R}{\sigma}\right)^{D} \tag{26}$$

or alternatively as $M = R^D$, if M is the mass of the cluster. In comparison with the $d = D$ case, where the uniform density of particles builds up a homogeneous cluster structure, when $D < d$, the density of the particles in the aggregate decreases with increasing size as a consequence of the non-homogeneous arrangement, since large amounts of open space are possible.

In general, we assume that the volume fraction ϕ of a system of N particles confined in a box of side L is: $\phi \sim N(\sigma/\Lambda)^d$, and that a growth mechanism produces a M-component system of clusters of particles with an effective volume fraction ϕ_{eff} that is given by:

$$\phi_{eff} \sim \sum_{i=1}^{M} n_i (R_i)^d \tag{27}$$

where n_i is the number of clusters of the i-th component N_i particles for cluster with $N = \sum_{i=1}^{M} n_i N_i$. Since the aggregates have a fractal structure, we have:

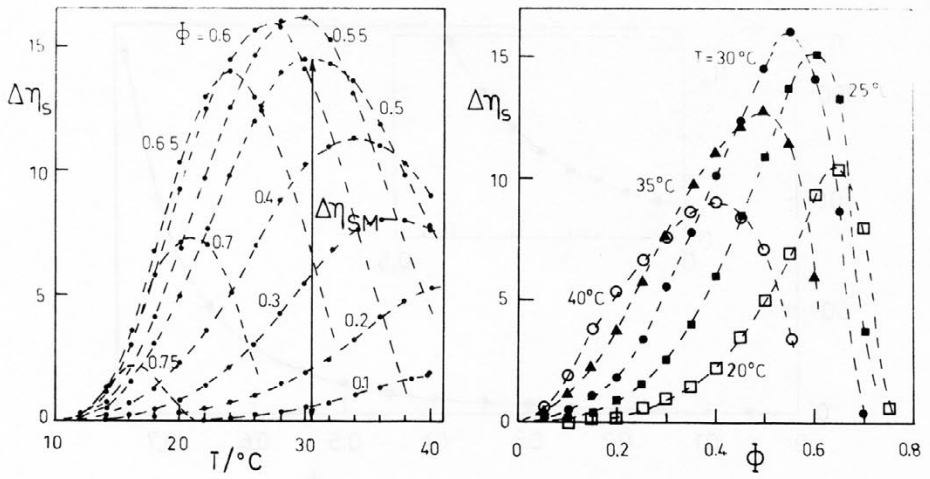

Figure 8 (a – left) Plot of the excess of viscosity, $\Delta\eta_S = \Delta\eta_{s,T} = \Delta\eta_{s,10}$, as a function of temperature and for different ϕ; (b – right) Plot of the excess of viscosity $\Delta\eta_s$, as a function of the water volume fraction ϕ, for temperatures of 20, 25, 30, 35, and 40 °C.

$$\frac{\phi_{\text{eff}}}{\phi} = N^{-1} \sum_{i=1}^{M} n_i N_i^{d/D} \tag{28}$$

If we have a single component system of n_M clusters with N_M particles per cluster, $(n_M N_M)/N = 1$, we obtain:

$$\frac{\phi_{\text{eff}}}{\phi} \sim \left(\frac{R_M}{\sigma}\right)^{(d-D)} \tag{29}$$

This result is exact for cluster by cluster diffusion limited aggregation[9,10] but it has been shown to hold as a good approximation for different models of kinetic growth,[49] as for example RLA which has been observed in our system.

Calling ϕ_s the volume fraction that corresponds to the largest possible cluster which, increasing ϕ, just spans the entire system, we can write:

$$\frac{\phi_{\text{eff}}}{\phi} \sim \left(\frac{R_M}{\sigma}\right)^{(d-D)} \sim \left(\frac{\Lambda}{\sigma}\right)^{(d-D)} \tag{30}$$

if $D < d$, then $\phi_S < \phi_m$. For systems with $\phi_S < \phi < \phi_m$, the dispersion is able to aggregate with a self-similar structure up to an upper cut-off length scale λ with $\lambda < \Lambda$. Packing constraints impose for the system a homogeneity with uniform density for length scales above λ and, therefore, for $\phi_S < \phi < \phi_m$, we have:

$$\frac{\phi_{\text{eff}}}{\phi} \sim \left(\frac{\lambda}{\sigma}\right)^{(d-D)} \sim \frac{\phi_{\text{eff}}}{\phi_S} \tag{31}$$

For $\phi \to \phi_m$, the packing causes $\lambda \to \sigma$ and $\phi_{\text{eff}} \to \phi$.

In this way, it is explained that in a disperse system where aggregation effects are present, $\phi_{\text{eff}} > \phi$ and ϕ_{eff} will display a maximum at ϕ_S. Through contribution η_2 of the hydrodynamic interaction of clusters, these results determine the shear viscosity of the system; hence, the effective volume fraction ϕ_{eff}, instead of ϕ and $\phi_{\text{eff}} > \phi$, must be used in this contribution if $D < d$. For aggregates with fractal structure, ϕ_{eff}/ϕ displays a maximum at the spanning volume fraction ϕ_S and the plot of shear viscosity *versus* volume fraction will display a local maximum at $\phi = \phi_S$.

The behaviour of our data (Figure 8b), is in qualitative agreement with a model that takes into account the viscosity contribution that arises from the formation of aggregates. In particular, the behaviour of the excess of viscosity $\Delta\eta_S$ for $T = 25$ °C is in complete agreement with the structural behaviour of the system studied by intensity light scattering measurements; in fact, these last measurements[17,33] give a well defined and extended fractal structure with $D = 2.1 \pm 0.05$ for $\phi \sim 0.58$ where $\Delta\eta_S$ shows its maximum value. Analogous behaviour can be observed from the mean linewidth data or initial decay rate $\langle\Gamma\rangle$ determined by means of the photon correlation spectroscopy[17] which shows the provided k^3 behaviour. This last result, easily understood as an obvious consequence of the well known relations,[50] for Brownian systems, among the linewidth and the viscosity ($\langle\Gamma\rangle \alpha \eta^{-1}$), allows us to relate the viscosity data to the fractal character of the systems.

This overall result, indicating that the clustering process is thermally activated, agrees with the physical properties of colloidal systems, as it has been recently shown by different theoretical and experimental[8,34] works using the general concepts of the DLVO theory. In fact, using some concepts developed in the initial part of this paper, we can obtain a definitive confirmation of this, considering in particular the above cited Chandrasekhar expression for the probability of escape to the potential barrier starting from the secondary minimum in $V(r)$.

In agreement with the structural model used, the effective volume fraction ϕ_{eff} and, therefore, the measured excess of viscosity $\Delta\eta_{SM}$, at the spanning volume fraction ϕ_S, can be considered to be connected with the number of N_i particles aggregated in a given cluster and, more directly, to the probability $P = 1/\tau_E$ that two single particles in the colloidal suspension stick together after escaping the potential barrier. In such terms we can write:

$$\Delta\eta_{SM} \propto N_i \propto \frac{1}{\tau} = \frac{(V_{min}'' \; V_{max}'')^{1/2}}{2\pi\beta} \; e^{-\Delta V/k_B T} \tag{6.a}$$

Such behaviour obviously holds only for $\phi \leq \phi_S$, while in the case in which $\phi_S < \phi < \phi_m$, packing constraint impose gradual fragmentation of the fractal structure up to the close packing structure with an Euclidean dimension $d = 3$. The corresponding sharp decrease, in this concentration region, in $\Delta\eta_{SM}$ can be related to such packing effects.

Figure 9 shows, for $\phi \leq \phi_S$ and for each volume fraction studied, the logarithmic plot of the excess viscosity maximum value $\Delta\eta_{SM}$ (Figure 8a) *versus* $1/T$. As it can be seen, the data well satisfy eq. (6.a) and the least square best fit gives $\Delta V \sim 8\, k_B T$. This value, for the potential barrier height, agrees with the one estimated for the interaction of two spherical particles[51] in a colloidal solution.

The other important finding that structure, and in particular the fractal one, can characterize collective dynamic quantities is represented by the results of Brillouin

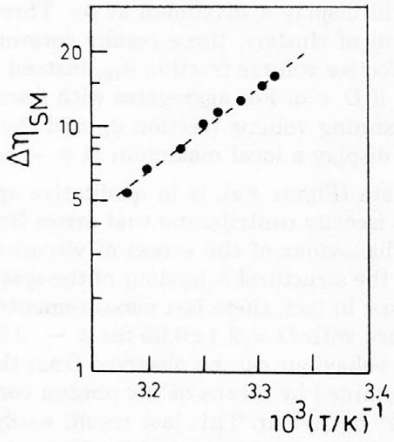

Figure 9. Logarithm plot of the maximum value of the excess of viscosity $\Delta\eta_s$, *vs.* $1/T$, for $\Delta\eta_{S,M}$ *vs* $1/T$, for $\phi \geq \phi_S$

scattering in dense AOT microemulsions. In fact, as we will show, hypersound velocity, with a well defined viscoelastic behaviour, reflects entirely the structural behaviour. As it is well-known, the elastic properties of the system are studied by measuring, from the Brillouin doublet, the speed of the longitudinal sound wave V. The dispersive behaviour of V as a function of ϕ for two temperatures (25 and 35 °C)[52] is shown in Figure 10, where the corresponding ultrasonic velocities V_{us} (5 MHz)[53] are also plotted for comparison. As it can be seen from Figure 10, the behaviour of V as a function of T is roughly the same of the oil phase for $\phi < 0.4$. More noticeably, we find that there is no appreciable difference between the V and V_{us} data; in contrast, for $\phi \sim 0.4$, there is a pronounced sound velocity dispersion, which is more significant at $T = 25$ °C. Such velocity dispersion can be related to the connected network formed by the droplets aggregation evidenced above. In our opinion, the overall velocity behaviour agrees very well with a model recently proposed by Ye *et al.*[54] for explaining sound propagation data in concentrated AOT-decane micellar solutions. In this model, the sound velocity of micellar solutions is associated to separated contributions from the dispersed phase and from the oil suspending medium. Velocity dispersion is related to a well defined transient network formed by the droplet aggregation. The short range attractive part of interparticle interaction has the dominant effect on high volume fractions where it gives rise to an aggregation process which forms a connected solid-like network. The dynamics of such structures reflects a well defined time behaviour with characteristic frequency dependence. For long time scales (low frequencies), the dynamics of the sys-

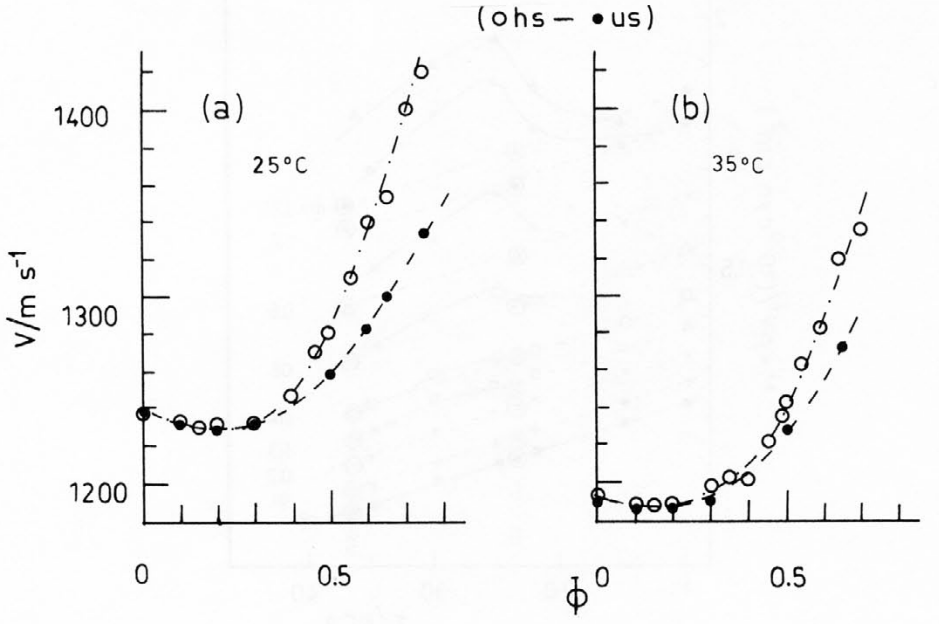

Figure 10. The volume fraction dependence of hypersonic velocity at two different temperatures (25 and 35 °); the corresponding ultrasonic velocities V_{us} (5 MHz), are plotted to show the dispersive behaviour of V

tem reflects a collection of non-interacting spheres in which shear stresses are relaxed; the particles behave like isolated particles undergoing Brownian motion and the observed sound velocity mainly reflects the physical behaviour of the suspending fluid. For short times, the solid-like network is able to support shear stresses and exhibits a finite elastic modulus. By increasing the concentration, the system rigidity (and, hence, the sound velocity) increases. The aggregation process is started by the same mechanism of increased connectivity between spherical droplets that is normally used to describe the behaviour of electrical conductivity in the percolation regime. Evidence for such structures has been obtained by different elastic and quasi-elastic light scattering experiments. Quasi-elastic[16,17] data show that the free diffusive motion of individual particles is inhibited because they are trapped in the structural cage formed by the nearest neighbouring droplets. The elastic scattering experiments,[16] giving the intensity profiles as a function of the exchanged wave vector k, show that such structures are fractals.

It is well known that in ultrasound experiments one can characterize the elastic properties of the system in terms of the complex longitudinal modulus $\tilde{M} = M' + iM''$, directly connected with the experimentally measured quantities,[55] *i.e.* velocity V and the absorption coefficient α. In particular, the velocity is associated to the real part

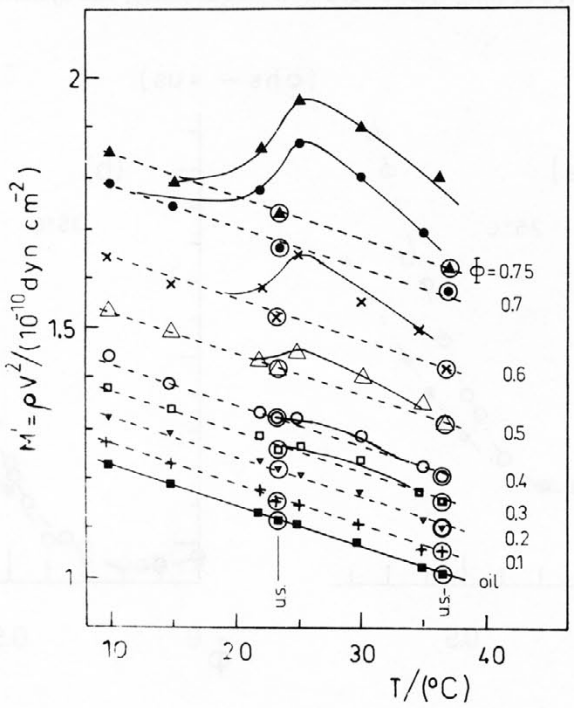

Figure 11. Temperature dependence of the real part of the longitudinal modulus M' at the investigated volume fractions. Values obtained from ultrasonic experiments are also reported.

of M by $V^2 = M'/\rho$ (ρ is the average density), while the damping of the sound wave per wavelength ($\alpha_\lambda = \alpha\lambda$) is related to M'' and M' by $\alpha_\lambda = \pi M''/M'$. Both quantities can be obtained by a Brillouin scattering experiment. As $\tilde{M}$ is given in terms of the bulk compressional modulus $\tilde{K}$ and of the shear modulus $\tilde{G}$ ($\tilde{M} = \tilde{K} + \tilde{G}4/3$), the obtained data are also sensitive to the shear rigidity of the system, although only the longitudinal properties are measured. In Figure 11, we report the temperature dependence of the real part of the longitudinal modulus M' for the investigated volume fractions. M' was evaluated by using the measured sound velocity and the mean density p. In the same figure, we also report the M' values measured in pure decane and those evaluated from ultrasonic velocity data at 5 MHz reported in ref. 53. As it can be observed, there is an overall increase of M' with increasing ϕ. At low concentrations ($\phi \leq 0.3$), the temperature behaviour of M' reflects that of the oil and the system exhibits no appreciable dispersion effects. In contrast, we can distinguish two temperature regions for higher volume fractions: a low temperature one (up to -20 °C) where the behaviour of the real part of the longitudinal modulus is still similar to that observed at low ϕ, and a high temperatures range $T \geq 20$ °C where noticeable dispersion effects, whose strength increases with ϕ, are observed.

The overall behaviour shown in Figure 11 can be explained within the framework of the two-fluid model proposed by Ye *et al.*.[54] According to this model, the real part of the longitudinal modulus of the system is a volume weighted contribution from the suspending oil and from the droplets, *i.e.*

$$M'(\omega.T,\phi) = (1 - \phi)\, M'_{OI}(\omega,T) + \phi\, M'_{DR}(\omega,T,\phi) \tag{32}$$

As the data in Figure 11 show that the T behaviour of the low frequency M' ($\omega \to 0$) is similar to $M'_{OI}(T)$, it follows that M'_{DR} (for $\omega \to 0$) depends smoothly on the temperature. In addition, Figure 11 shows that $M'_{OI}(T)$ is frequency independent and, therefore, the ω dependence of M' is mainly related to $M'_{DR}(\omega)$, *i.e.* to the dynamics of the structural arrangements of the droplets. A more detailed inspection of the experimental data shows that this structural process is thermally activated. As it is common for viscoelastic systems, we can distinguish between the long and short time behaviour of the system by reporting the difference $\Delta M'$ between the longitudinal modulus measured at high frequencies (hypersonic values) and that measured at low frequencies (ultrasonic values) for each ϕ. As it is well known, assuming that hypersonic and ultrasonic data represent, respectively, properties in the infinite and zero frequency limits, this difference can be written as

$$\Delta M' = M'_\infty - M'_0 = \rho\,(V^2 - V_{us}^2) = K_r + 4G_\infty/3$$

where K_r and G_∞ represent the relaxational compressional modulus ($K_r = K_\infty - K_0$) and the high frequency value of the shear modulus, respectively. In Figure 12, we plot $\Delta M'$ as a function of T for $\phi \geq 0.3$; in the same figure, the experimentally found temperatures corresponding to the percolation threshold for each ϕ are indicated by arrows.[18] As it can be seen, the temperatures of our $\Delta M'$ maxima closely correspond to the percolation threshold temperatures. In addition, the different trends exhibited by $\Delta M'$ below and above the threshold seem to indicate a different structural behaviour. This, in turn, could be related to the transition of the system from a dynamic to a static percolation regime, as shown by different experimental measurements.[18] In con-

clusion, we emphasize that these findings have been obtained directly from the experimental data and are independent of any model. Figure 12, showing a clear correlation between our results and the percolation process, suggests that the velocity dispersion is strongly connected with structural processes. Other measurements are necessary to clarify this last aspect and to link the presence of the solid-like network with the percolation theory in a quantitative way. In particular, this applies to the changing of the strength of velocity dispersion and relaxation frequencies by using oils of different carbon chain lengths.

Finally, we show that analogous results can be obtained by calorimetric data analyzed within the framework of a two-fluid model, as it has been done for viscosity and hypersound velocity results. Figure 13 presents a plot, as a function of the droplet volume fraction ϕ, of two measurements of specific heat at constant pressure C_p for $T = 23$ °C.[56] These data, starting from the decane value ($\phi = 0$), show a monotonic increase as a function of the concentration due to the continuous increase in the disperse phase (number of droplets); structural or dynamic effects can be extracted after normalization to the number of droplets. If, in analogy of the two fluid model used for hypersound and viscosity data, the measured C_p is considered as the sum of two different contributions, the following relation can be written:

$$C_P(\phi) = C_{PO}(1 - \phi) + C_{PD}\phi \tag{33}$$

where $C_{PO}(1-\phi)$ is the contribution to the measured specific heat at the ϕ concentration due to the oil phase (in our case C_{PO} is the decane specific heat) and C_{PD} is the

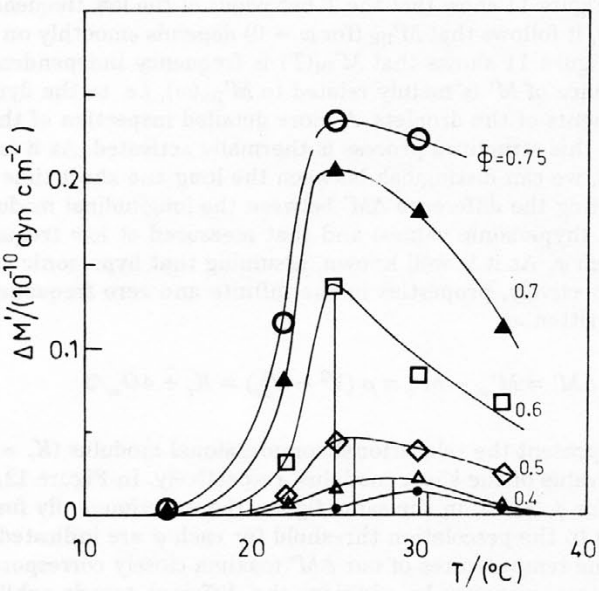

Figure 12. The relaxational longitudinal modulus $\Delta M'$ as a function of T for $\phi \geq 0.3$; the arrows indicate the percolation threshold temperatures.

contribution of the »system« droplets. This normalization is made in order to obtain only the contributions to the specific heat due to structural effects.

Figure 14 shows the result of such a normalization plotting C_{PD} as a function of ϕ for different temperatures;[56] it is clear that this quantity is strongly dependent on

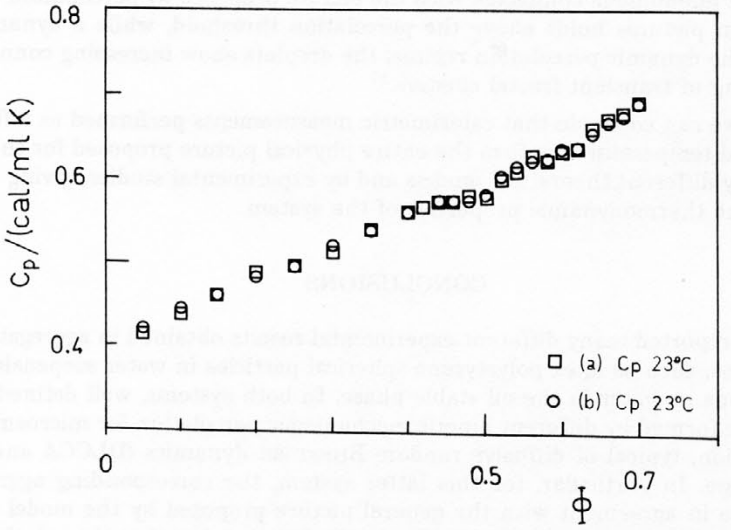

Figure 13. Plot, as a function of the droplet volume fraction ϕ, of two different sets of measurements of constant pressure specific heat C_p, for T = 23 °C.

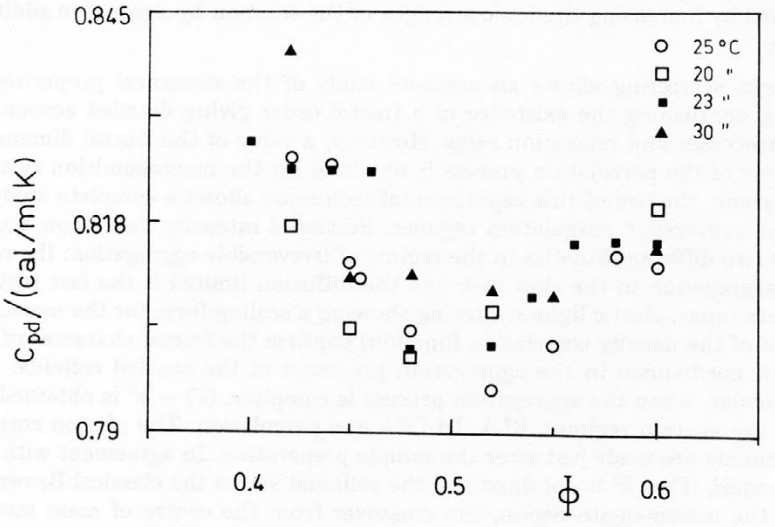

Figure 14. Plot of C_{PD}, the contribution to c_P due to the dispersed phase, as a function of ϕ for different temperatures.

the packing fraction ϕ. As it can be seen, we have a defined minimum in C_{PD} in the ϕ range 0.45 – 0.55. Taking that this is the concentration range where, at the explored temperatures, percolation takes place, we can easily ascribe such minima in the measured specific heat to structural processes. In particular, the observed minima can be ascribed to entropy variations, ($C_P = (\partial S/\partial T)_P$), for the ordering processes induced by the structural phenomena connected with the picture proposed by percolation.[18] A static percolation pictures holds above the percolation threshold, while a dynamic one below it. In the dynamic percolation regime, the droplets show increasing connectivity in the building of transient fractal clusters.[17]

Finally, we can conclude that calorimetric measurements performed as a function of density and temperature confirm the entire physical picture proposed for these systems by many different theoretical models and by experimental studies, giving new insights into the thermodynamic properties of the system.

CONCLUSIONS

We have reported many different experimental results obtained in aggregating dispersed systems, such as latex polystyrene spherical particles in water suspensions and microemulsions in water in the oil stable phase. In both systems, well defined fractal structures are formed by different kinetic mechanisms: percolation for microemulsions and aggregation, typical of diffusive random Brownian dynamics (DLCCA and RLA), for polystyrene. In particular, for this latter system, the corresponding aggregation properties are in agreement with the general picture proposed by the model for colloidal stability described by the DLVO theory. In fact, by changing the solution ionic strength, it is possible to observe both reversible flocculation, where the colloid is in a metastable state for a very long period of time, and the irreversible coagulation which presents two different regimes, a fast and a slow one. The irreversible coagulation is obtained by increasing the ionic strength of the solution by successive addition of electrolyte.

Elastic light scattering allows an accurate study of the structural properties of these systems, confirming the existence of a fractal order giving detailed account of aggregation processes and relaxation rates. However, a value of the fractal dimension D characteristic of the percolation process is obtained for the macroemulsion system. As for polystyrene, the use of this experimental technique allows a complete study of reversible and irreversible coagulation regimes. Scattered intensity data show unambiguously the two different kinetics in the regime of irreversible aggregation: the reaction limited aggregation in the slow case and the diffusion limited is the fast regime. Dynamical data (quasi-elastic light scattering showing a scaling form for the measured first cumulant of the density correlation function) confirm the fractal character of the kinetic-growth mechanism in the aggregation processes of the studied colloidal systems. In particular, when the aggregation process is complete, $\langle\Gamma\rangle \sim k^3$ is obtained for the different aggregation regimes, RLA, DLCCA and percolation. The photon correlation measurements are made just after the sample preparation. In agreement with the theoretical models, $\langle\Gamma\rangle \sim k^2$ is obtained and the colloidal shows the classical Brownian diffusion. In the intermediate region, the crossover from the centre of mass motion to the cluster internal motion can be explored. When the aggregation process is complete, the comparison of the order of magnitude of the measured relaxation rate $\langle\Gamma\rangle/k^2$ enables an estimate of the cluster dimensions.

Thermodynamical measurements make it possible to explore the effects of aggregation mechanism on collective quantities such as viscosity, sound propagation and specific heat. It is possible to study the contribution to them of the attractive interactions through the growth mechanism involving the formation of long-range fractal structures. More precisely, the use of a two-fluid model shows the viscosity contribution due to attractive interactions, given indirectly by the formation of percolating fractal structures, and explains the presence of well defined maxima in the experimental data. Such maxima can be connected with the properties of the aggregation process and, in particular, with its fractal geometry; the homogeneity in the density correlation function, which is a consequence of the self-similarity of the built-up structures, allows us to define an effective volume fraction ϕ_{eff} which for $D < d$ is $\phi_{\text{eff}} > \phi$. Therefore, as a consequence of the aggregation process, the increase in the concentration of the system causes ϕ_{eff}/ϕ to increase up to the spanning volume fraction ϕ_S: after that, the packing constrains remove the structure with a sharp decrease in ϕ_{eff}, approaching the close volume fraction $\phi_{\text{eff}} \to \phi$. Such behaviour is reflected in the shear viscosity which, in a plot against volume fraction, displays a maximum at $\phi = \phi_S$.

Finally, a proper analysis of viscoelastic properties of the investigated systems, in terms of the reported effective medium approach, gives new insights into the properties of sound propagation in these systems, indicating again that the observed effects are related to the dynamics of the aggregation processes. In these terms it is possible to consider the sound velocity of the aggregating solutions associated to the separated contributions from the dispersed phase and from the suspending medium. Velocity dispersion can be connected to a well defined transient network formed by the droplet aggregation. The short range attractive part of the interparticle interaction becomes the dominant effect at high concentrations or temperatures where it gives rise to the aggregation which forms a connected solid-like network. The dynamics of such structures reflects a well defined time behaviour with a characteristic frequency dependence. For long time scales (low frequencies), the dynamics of the system reflects a collection of non- interacting spheres in which shear stresses are relaxed: the particles behave like isolated particles undergoing Brownian motion and the observed sound velocity mainly reflects the physical behaviour of the suspending fluid. For short times, the solid-like network is able to support shear stresses and exhibits a finite elastic modulus. By increasing the concentration, the system rigidity (and then the sound velocity) increases. Such behaviour agrees with the reported results of different elastic and quasi-elastic light scattering experiments. Definitive validity of this approach to the study of thermodynamical data is given by the findings obtained from calorimetric measurements.

We conclude with a comment on the general validity of the DLVO theory on colloidal stability; in fact, all the reported data obtained by several different experimental techniques are consistent with this model, clarifying the significant role of the interparticle potential. However, there are still many open problems concerning the aggregation processes in colloidal systems. For example, the molecular origin of the presence of two different growth mechanisms such as RLA and the DLCCA in the phase of irreversible flocculation is not clear; furthermore, the correlations between percolation or aggregation processes, with defined fractal structures, and the viscoelastic behaviour of these systems should be studied in a more quantitative way. Another problem is the so-called slow dynamics, *i.e.* the peculiar long time behaviour typical of the class of complex fluids like those presented here.

REFERENCES

1. H. J. Herrmann in *On growth and form,* ed. by H. E. Stanley and N. Ostrowski, NATO ASI series Nijhoff Dordrecht, 1986.
2. M. V. Smoluchowski, *Phys. Z.* **17** (1916) 557.
3. E. J. Verwey and J. Th. G. Overbeek, »*Theory of the Stability of Lyophobic Colloids*« (Elsevier, Amsterdam, 1948.
4. H. E. Stanley, in Ref. 1.
5. T. A. Witten and L. M. Sander, *Phys. Rev. Lett.* **47** (1981) 1400.
6. B. Mandelbrot in »*Fractals, Form and Dimension*« Freeman, San Francisco, 1977.
7. R. H. Ottewill, *Sp. Rep. Chem. Soc. Colloid Sci.* **1** (1973) 175.
8. G. Bolle, C. Cametti, P. Codestafano, and P. Tartaglia, *Phys. Rev. A* **35** (1987) 837; C. Canmetti, P. Codastefano, and P. Tartaglia, *Phys. Rev. A* **36** (1987) 4916.
9. P. Meakin, *Phys. Rev. Lett.* **51** (1983) 119.
10. M. Kolb, T. Jullen, and R. Botet, *Phys. Rev. Lett.* **51** (1983) 1123.
11. D. A. Weitz, J. S. Huang, M. Y. Lin, and J. Sung, *Phys. Rev. Lett.* **53** (1984) 1657; **54** (1985) 141.
12. C. Aubert and D. Cannel, *Phys. Rev. Lett.* **56** (1986) 738.
13. P. Meakin and M. Muthukumar, *J. Chem. Phys.* **91** (1989) 3212.
14. B. V. Derjajuin and L. Landau, *Acta Phys. Chim. Debricina* **14** (1941) 633.
15. M. Kotlarchyk, S. H. Chen, J. S. Huang, and M. W. Kim, *Phys. Rev. A* **29** (1984) 2054; E. Y. Sheu, S. H. Chen, J. S. Huang, and J. C. Sung, *Phys. Rev. A* **39** (1989) 5867.
16. S. H. Chen and J. S. Huang, *Phys. Rev. lett.* **55** (1985) 1888.
17. S. Magazu', D. Majolino, G. Maisano, F. Mallamace, and N. Micali, *Phys. Rev. A* **40** (1989) 2643.
18. C. Cametti, P. Codastefano, P. Tartaglia, J. Rouch, and S. H. Chen, *Phys. Rev. Lett.* **64** (1990) 1461; C. Cametti, P. Codastefano, Di Biasio, P. Tartaglia, and S. H. Chen,*Phys. Rev. A* **40** (1989) 1962.
19. D. Stauffer, *Phys. Rep.* **54** (1979) 1.
20. D. Stauffer, in ref. 1
21. D. W. Schaefer and C. C. Han, in *Dynamic Light Scattering*, edited by R. Pecora (Plenum, New York, 1985).
22. H. C. Hamaker, *Physica* **4** (1937) 1058.
23. S. Chandrasekhar, *Rev. Mod. Phys.* **15** (1943) 1.
24. D. Eagland in »*Water a Comprehensive Treatise*« edited by F. Franks Vol. 5 (Plenum, New York, 1975).
25. I. E. Dzayaloshinskii, E. M. Lifshitz, and L. P. Pitaevskii, *Advan. Phys.* **10** (1959) 165; M. J. Vold, *J. Colloid Sci.* **16** (1961) 1.
26. B. W. Ninham and V. A. Pasergian, *Biophysic J.* **10** (1970) 646; *J. Chem. Phys.* **53** (1970) 3398.
27. D. W. Schaefer, *J. Chem. Phys.* **66** (1977) 3980.
28. W. Hess and R. Klein, *Advan. Phys.* **32** (1983) 173.
29. T. Okubo, *J. Chem. Phys.* **87** (1987) 6733.
30. R. Richterl, L. M. Sander, and Z. Cheng, *J. Colloid Interface Sci.* **100** (1984) 203.
31. J. E. Martin and J. Ackerson, *Phys. Rev. A* **31** (1985) 1180.
32. J. Teixeira, in ref. 1; S. H. Chen and J. Teixeira, *Phys. Rev. Lett.* **57** (1986) 2583.
33. P. Tartaglia, J. Rouch, and S. H. Chen, *Dynamic Slowing Down in Dense Percolating Microemulsion* to be published).
34. D. Majolino, F. Mallamace, P. Migliardo, N. Micali, and C. Vasi, *Phys. Rev. A* **40** (1989) 4665.
35. J. C. Slater and J. G. Kirkwood, *Phys. Rev. A* **37** (1931) 682.
36. R. M. Cornell, J. W. Goodwin, and R. H. Ottewill, *J. Colloid Interface Sci.* **71** (1979) 254.
37. B. J. Berne and R. Pecora, »*Dynamic Light Scattering*« (Wiley, New York, 1975).
38. J. E. Martin and D. W. Shaefer, *Phys. Rev. Lett.* **53** (1984) 2457.
39. W. van Saalos, *Physica* **147 A** (1987) 280.
40. S. Magazu', G. Maisano, F. Mallamace, and N. Micali, *Phys. Rev. A* **39** (1989) 4195.
41. R. Giordano, F. Mallamace, N. Micali, F. Wanderlingh, G. Baldini, and S. Doglia, *Phys. Rev. A* **28** (1983) 3581; N. Parthasarathy and K. S. Schmitz, *Biopolymers* **19** (1980) 1655.

42. D. Majolino, F. Mallamace, N. Micali, and S. Venuto, *Phys. Rev. A* **42** (1990) 7330.
43. R. C. Ball and P. Richmond, *Phys. Chem. Liq.* **9** (1980) 99.
44. J. Peyrelasse, M. Moha-Ouchane, and C. Bined, *Phys. Rev. A* **38** (1988) 4155.
45. M. J. Grimson and G. C. Barker, *Europhys. Lett.* **3** (1987) 511.
46. R. Buscall, J. W. Goodwin, M. W. Hawkins, and R. H. Ottewill, *J. Chem. Soc., Faraday Trans. I* **78** (1982) 2889.
47. A. Einstein, *Ann. Phys. (Leipzig(* **19** (1906) 289.
48. J. S. Huang, *J. Chem. Phys.* **82** (1985) 480.
49. See for example »*Scaling Phenomena in Disordered System*« edited by R. Pynn and A. Skjeltorp (Plenum, New York 1985).
50. P. N. Pusey and R. J. A. Tought in »*Dynamic Light Scattering*« edited by R. Pecora (Plenum, New York, 1985).
51. D. Eagland in »*Water a Comprehensive Treatise*« edited by F. Franks, Vol. 5 (Plenum, New York, 1975).
52. F. Mallamace, N. Micali, C. Vasi, and G. D' Arrigo, *Phys. Rev. A* **43** (1991) 5710.
53. C. Cametti, P. Codastefano, G. D'Arrigo, P. Tartaglia, J. Rouch, and S. H. Chen, *Phys. Rev. A* **42** (1990) 3421.
54. L. Ye, D. A. Weitz, Ping Scheng, S. Bhattacharya, J. S. Huang, and M. J. Higgins, *Phys. Rev. Lett.* **64** (1989) 263.
55. T. A. Litovitz and C. M. Davis in *Physical Acoustic* edited by W. P. Mason (Academic Press, New York, 1965).
56. F. Mallamace, N. Micali, S. Squadrito, P. Salvetti, and S. Veronesi, *Phys. Rev. Lett.* (submitted).

SAŽETAK

Fraktalne strukture i njihovi efekti na dinamiku supramolekulskih agregata mjerenjima rapršenja svjetla i termodinamičkih svojstava

F. Mallamace i N. Micali

Izvještava se o podacima raspršenja svjetla, viskoznosti, širenja zvuka i kalorimetrije, u disperznim sustavima, koji reagiraju. To su koloidne suspenzije specifičnih polistirenskih lateksa u mikroemulzijama voda-ulje. Elastično i kvazielastično raspršenje svjetla daje direktne informacije o agregiranim nakupinama kao fraktalnim strukturama, te o odgovarajućim različitim kinetičkim mehanizmima. Posebno dinamički podaci potvrđuju predodžbu načinjenu na temelju podataka o intenzitetu elestičnog raspršenja svjetla, te pokazuju dobro definirano skaliranje u mjerenim prosječnim širinama linija, i time dozvoljavaju grubu procjenu dimenzije nakupina. Svi termodinamički podaci diskutirani pomoću dvo-fluidnog modela (suspendirajući fluid i disperzni sustav koji međusobno djeluju) pokazuju da glavnu ulogu igraju privlačna međudjelovanja čestica. Tipične pojave koje pokazuju podaci o viskoznosti, podaci o toplinskim kapacitetima, te o viskoelastičnom ponašanju ispitivanih disperznih sustava, mogu se povezati sa strukturnim redom dugog dometa, nastalim uslijed fraktalnih agregacijskih procesa. Svi eksperimentalni podaci u skladu su s DLVO-teorijom koloidne stabilnosti.